Performance Analysis of a Rate-Adaptive Dual-Branch Switched Diversity System

Bengt Holter* and Geir E. Øien†
*SINTEF ICT, Communication Systems
O. S. Bragstads plass 2C, N-7465 Trondheim, Norway, Email: bengt.holter@sintef.no
†Norwegian University of Science and Technology, Dept. of Electronics and Telecommunications
O. S. Bragstads plass 2B, N-7491 Trondheim, Norway, Email: geir.oien@iet.ntnu.no

***Abstract*— In this paper, a performance analysis of a dual-branch switched diversity system operating on identically distributed Nakagami-m fading channels is presented. An adaptive coded modulation (ACM) scheme is employed to increase the spectral efficiency of the system. The ACM scheme consists of a set of multidimensional trellis codes originally designed for additive white Gaussian noise channels, where the codes are based on quadrature amplitude modulation (QAM) signal constellations of varying size. The performance is evaluated by assuming perfect channel knowledge at the receiver and instantaneous feedback of channel state information, conveyed from the receiver to the transmitter on a zero-error feedback channel. Both spatially uncorrelated and correlated antenna branches are considered. The optimal switching threshold in terms of maximizing the average spectral efficiency is identified in the case of uncorrelated antenna branches.**

I. Introduction

Adaptive modulation is an efficient transmission scheme to simultaneously achieve both high spectral efficiency and a low bit error rate (BER) in a wireless communication system. The basic principle is to utilize channel state information (CSI) conveyed from the receiver to the transmitter to adapt to changing channel conditions by transmitting with high information rates under favorable channel conditions, and reducing the information rate in response to channel degradation.

In [1], [2], a method for assessing performance merits of an adaptive *coded* modulation (ACM) system is employed to evaluate the average spectral efficiency (ASE) of a rate-adaptive coding scheme utilizing a set of multidimensional trellis codes originally designed for additive white Gaussian noise (AWGN) channels. The analysis is based on a single-input multiple-output (SIMO) channel model with statistically independent and identically distributed (i.i.d.) Rayleigh fading channels. Perfect coherent detection is assumed and maximum ratio combining (MRC) is employed to maximize the received signal-to-noise ratio (SNR).

The MRC receiver is frequently used in the literature for analysis purposes as a benchmark receiver, since it represents the optimal (in a maximum SNR sense) diversity scheme in the absence of interference.[1] However, it also represents the diversity scheme with the highest complexity, since it requires continuous monitoring of all channel fading parameters and separate receiver chains for all the branches. As a result, less complex diversity schemes are typically used in practice. Our motivation for the present paper is to investigate the performance of the ACM scheme in [1], [2] when using a simpler combining technique than MRC. In particular, a dual-branch *switched diversity* combiner is used, and a switch-and-stay (SSC) combining strategy is applied [4].

In [5], a discrete-time model using a SSC strategy was introduced to develop a performance analysis of a dual-branch switched diversity system, using noncoherent frequency shift keying operating on independent Rayleigh channels. The analysis in [5] was later extended to include a Nakagami-m fading model [6]. In [7], a slightly different switching strategy than [5] was presented for both uncorrelated and correlated branches, leading to closed-form solutions for the optimal switching thresholds in a minimum probability of error sense. Building on the framework developed in [5], [7] and [8], an extensive performance analysis of a dual-branch switched diversity system was presented in [4], deriving new generic and exact analytical results for the performance of SSC when used in conjunction with several M-ary signal constellations. Recently, the analysis in [4] was extended to a multibranch switched diversity systems [9]. Additional work, specifically related to the performance of dual-branch switched diversity receivers can be found in [10]–[15].

All the referenced papers on switched diversity limit their studies to systems using only a single fixed signal constellation. Indeed, to our knowledge, a performance analysis of a switched diversity system utilizing an ACM scheme has not yet been reported in the literature.[2] However, this is of practical interest, since the introduction of some diversity in the system will lower the probability of the deep fades for which channel prediction, necessary for the use of ACM, becomes too unreliable. In an attempt to fill this gap, and building on the framework presented in [1], [2], a performance analysis of an ACM scheme is therefore presented in this paper, with a dual-branch switched diversity combiner being used at the receiver.

[1] When interference is present, the optimal combining scheme is denoted an optimum combiner, maximizing the instantaneous received signal-to-interference plus noise ratio (SINR) [3]

[2] In [16], an *uncoded* adaptive modulation scheme is utilized to jointly minimize the number of *combined* diversity branches while providing the highest possible spectral efficiency.

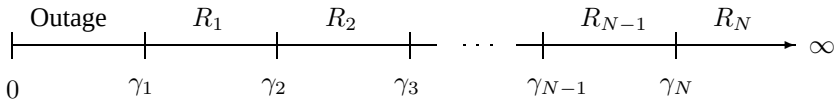


Fig. 1. The SNR range is split into $N+1$ bins. When the instantaneous SNR falls in the lowest interval, an outage occurs; whereas in the upper N intervals, a code with spectral efficiency R_n is employed.

II. System and channel model

A single user dual-branch SIMO system operating on two i.i.d. Nakagami-m fading channels is considered. The transmission rate on the wireless link is adaptively adjusted by utilizing a rate-adaptive coding scheme, using a set of N multi-dimensional trellis codes originally designed for AWGN channels. The codes are based on quadrature amplitude modulation (QAM) signal constellations, and rate adaptation is performed by splitting the received SNR range into $N+1$ fading regions (bins) as depicted in Figure 1. The set $\{\gamma_n\}_{n=1}^{N}$ contains the lower thresholds of the N fading regions, selected such that a target BER—denoted BER_0—is achieved for each available code in the rate-adaptive scheme.[3] Let γ_{ssc} denote the SNR per symbol at the output of the SSC combiner, and let γ_T denote the predetermined switching threshold. When γ_{ssc} falls within fading region n ($\gamma_n \le \gamma_{ssc} < \gamma_{n+1}$), the associated CSI, i.e. the fading region index n, is sent back to the transmitter through a dedicated feedback channel. Based on the reported CSI, the transmitter adapts its transmission rate according to the quality of the channel, by transmitting with a signal constellation realizing a spectral efficiency of R_n. If $0 \le \gamma_{ssc} < \gamma_1$, no information is transmitted (outage). In this paper, the following three idealized assumptions are employed: (i) the receiver has perfect channel knowledge (ii) instantaneous feedback (iii) the feedback channel is zero-error.

For i.i.d. channels, the probability density function (PDF) of the output SNR of a dual-branch SSC combiner may be written as [4]

$$p_{\gamma_{ssc}}(\gamma) = \begin{cases} P_\gamma(\gamma_T) \cdot p_\gamma(\gamma) & \gamma < \gamma_T \\ (1 + P_\gamma(\gamma_T)) \cdot p_\gamma(\gamma) & \gamma \ge \gamma_T \end{cases} \tag{1}$$

where $p_\gamma(\gamma)$ and $P_\gamma(\gamma)$ are the PDF and the cumulative distribution function (CDF) of the output SNR per symbol γ for a single branch receiver, respectively. In Table I, expressions for the PDF and CDF are presented for the Nakagami-m fading model, where $\overline{\gamma}$ represents the average SNR on a single channel, $\beta = \overline{\gamma}/m$, $\Gamma(\cdot)$ is the gamma function [17, Sec. 8.31], and $\Gamma(\cdot,\cdot)$ is the complementary incomplete gamma function [17, Sec. 8.35].

III. ASE and BER analysis

The ASE [bits/s/Hz] of the system is obtained as a weighted sum of the spectral efficiencies of each individual code, i.e. $\text{ASE} = \sum_{n=1}^{N} R_n P_n$, where $P_n = \int_{\gamma_n}^{\gamma_{n+1}} p_{\gamma_{ssc}}(\gamma) d\gamma$ is the probability that code n is used. The average BER (averaged over all codes and all SNRs) is given as the average number of bits in error, divided by the average number of bits transmitted [2]

$$\overline{\text{BER}} = \frac{\sum_{n=1}^{N} R_n \cdot \overline{\text{BER}}_n}{\sum_{n=1}^{N} R_n \cdot P_n}, \tag{2}$$

where $\overline{\text{BER}}_n$ is the average BER experienced when code n is applied. It is obtained as $\overline{\text{BER}}_n = \int_{\gamma_n}^{\gamma_{n+1}} \text{BER}_n p_{\gamma_{ssc}}(\gamma) d\gamma$, where $\text{BER}_n = a_n \exp\{-b_n \gamma / M_n\}$ is the instantaneous BER experienced for code n, and a_n and b_n are code-dependent constants found by least-square fitting to simulated data on AWGN channels. Since the expression for BER_n is invertible, the thresholds in the set $\{\gamma_n\}_{n=1}^{N}$ can be identified as $\gamma_n = (M_n/b_n)\ln(a_n/\text{BER}_0)$. In Table II, values for a_n, b_n, M_n, and γ_n are summarized for the target $\text{BER}_0 = 10^{-4}$ and $N = 8$ (number of codes used in the numerical examples). Restricting γ_T to be larger than γ_1, P_n may in general be divided into three parts:[4]

$$P_n = \begin{cases} P_n^{\text{left}} &= \mathcal{I}(n) \cdot P_\gamma(\gamma_T) & \gamma_{n+1} < \gamma_T \\ P_n^{\text{in}} &= \mathcal{I}_{\gamma_T}(n) + P_n^{\text{left}} & \gamma_n < \gamma_T \le \gamma_{n+1} \\ P_n^{\text{right}} &= \mathcal{I}(n) + P_n^{\text{left}} & \gamma_T \le \gamma_n \end{cases}, \tag{3}$$

where $\mathcal{I}(n) = \int_{\gamma_n}^{\gamma_{n+1}} p_\gamma(\gamma) d\gamma$ and $\mathcal{I}_{\gamma_T}(n) = \int_{\gamma_T}^{\gamma_{n+1}} p_\gamma(\gamma) d\gamma$.

The superscripts in (3) are introduced to distinguish between the different expressions for P_n, depending on the placement

TABLE I

PDF and CDF of the SNR per symbol γ for a single Nakagami-m fading channel

Model	Parameter	PDF ($p_\gamma(\gamma)$)	CDF ($P_\gamma(\gamma)$)
Nakagami-m	$m \ge \frac{1}{2}$	$\frac{\gamma^{m-1} e^{-\gamma/\beta}}{\beta^m \Gamma(m)}$	$1 - \frac{\Gamma(m,\gamma/\beta)}{\Gamma(m)}$

TABLE II

Parameters a_n and b_n with thresholds γ_n for $\text{BER}_0 = 10^{-4}$.

n	M_n	a_n	b_n	γ_n [dB]
1	4	188.7471	9.8118	7.7
2	8	288.8051	6.8792	12.4
3	16	161.6898	7.8862	14.6
4	32	142.6920	7.8264	17.6
5	64	126.2118	7.4931	20.8
6	128	121.5189	7.7013	23.7
7	256	79.8360	7.1450	26.9
8	512	34.6128	6.9190	29.7

[3] $\gamma_{N+1} = \infty$.

[4] For simplicity, γ_T is restricted not to reside within the interval range $0 \le \gamma < \gamma_1$ (outage region).

of γ_T on the SNR axis in Figure 1. For the fading bins located to the left of γ_T, $P_n = P_n^{\text{left}}$. For the fading bin containing γ_T, $P_n = P_n^{\text{in}}$. For the fading bins located to the right of γ_T, $P_n = P_n^{\text{right}}$. Similarly, $\overline{\text{BER}}_n$ can be expressed as

$$\begin{array}{lcll} \overline{\text{BER}}_n^{\text{left}} & = & \mathcal{J}(n) \cdot P_\gamma(\gamma_T) & \gamma_{n+1} < \gamma_T \\ \overline{\text{BER}}_n^{\text{in}} & = & \mathcal{J}_{\gamma_T}(n) + \overline{\text{BER}}_n^{\text{left}} & \gamma_n < \gamma_T \leq \gamma_{n+1} \\ \overline{\text{BER}}_n^{\text{right}} & = & \mathcal{J}(n) + \overline{\text{BER}}_n^{\text{left}} & \gamma_T \leq \gamma_n \end{array}, \quad (4)$$

where $\mathcal{J}(n) = \int_{\gamma_n}^{\gamma_{n+1}} a_n e^{-\frac{b_n \gamma}{M_n}} p_\gamma(\gamma) d\gamma$ and $\mathcal{J}_{\gamma_T}(n) = \int_{\gamma_T}^{\gamma_{n+1}} a_n e^{-\frac{b_n \gamma}{M_n}} p_\gamma(\gamma) d\gamma$. The expressions in (3) and (4) are applicable to any fading distribution.

In the following, the index $q \in [1, 2, \cdots, N]$ is used to indicate the fading bin in which γ_T is placed. In particular, $q = n$ if $\gamma_n \leq \gamma_T \leq \gamma_{n+1}$. For a system operating on i.i.d. Nakagami-m fading channels, the ASE and the average BER may then be written compactly as

$$\text{ASE} = (R_q - \mathcal{A}_1)\overline{\Gamma}(m, \gamma_T/\beta) + \mathcal{T}_q, \quad (5)$$

and

$$\overline{\text{BER}} = \frac{R_q \mathcal{C}_q \overline{\Gamma}(m, \mu_q \gamma_T) - \mathcal{B}_1 \overline{\Gamma}(m, \gamma_T/\beta) + \mathcal{S}_q}{(R_q - \mathcal{A}_1)\overline{\Gamma}(m, \gamma_T/\beta) + \mathcal{T}_q}, \quad (6)$$

respectively. The expressions involved are defined as $\mathcal{A}_1 = \sum_{n=1}^{N} R_n \mathcal{I}(n)$, $\mathcal{B}_1 = \sum_{n=1}^{N} R_n \mathcal{J}(n)$, $\mathcal{T}_q = \mathcal{A}_1 + \mathcal{A}_{q+1} - R_q \overline{\Gamma}(m, \gamma_{q+1}/\beta)$, $\mathcal{S}_q = \mathcal{B}_1 + \mathcal{B}_{q+1} - R_q \mathcal{C}_q \overline{\Gamma}(m, \mu_q \gamma_{q+1})$, $\mathcal{A}_{q+1} = \sum_{n=q+1}^{N} R_n \mathcal{I}(n)$, $\mathcal{B}_{q+1} = \sum_{n=q+1}^{N} R_n \mathcal{J}(n)$, $\mathcal{C}_q = \frac{a_q}{(\beta \mu_q)^m}$, and $\mu_q = (b_q \beta + M_q)/(M_q \beta)$.[5] Note that both (5) and (6) are functions of q, γ_T, $\overline{\gamma}$, and m.

IV. Maximizing the ASE

In the following, γ_T which maximizes the ASE within a single fading bin q is determined by assuming that $\overline{\gamma}$ and m are fixed. Then, based on this result, the optimal fading bin q^* and the associated optimal threshold γ_T^*, maximizing the ASE over *all* fading bins, is determined. Since the ASE is a key performance measure only when the system is operating at acceptable BER levels (below BER_0), the optimization of (5) can formally be defined as an optimization problem with a side constraint: *maximize* ASE *subject to* BER $\leq \text{BER}_0$.

However, since BER $\leq \text{BER}_0$ is used as a design criteria to obtain the thresholds $\{\gamma_n\}_{n=1}^N$, both the instantaneous and the average BER are guaranteed to be lower than or equal to BER_0 as long as perfect channel knowledge is assumed [18]. Hence, the side constraint is already introduced, and the ASE in (5) may be optimized as if it represented an unconstrained optimization problem. The partial derivative of (5) with respect to γ_T is equal to

$$\frac{\partial \text{ASE}}{\partial \gamma_T} = -(R_q - \mathcal{A}_1) \cdot \mathcal{G}_{\gamma_T}(m, \beta), \quad (7)$$

where $\mathcal{G}_{\gamma_T}(m, \beta) = \frac{\gamma_T^{m-1} e^{-\gamma_T/\beta}}{\beta^m \Gamma(m)}$. Since $\mathcal{G}_{\gamma_T}(m, \beta) > 0$ for $1/2 \leq m \leq 4$, $\overline{\gamma} \geq 0$ dB, and $0 < \gamma_T < \infty$, the derivative has the following properties when $\gamma_q \leq \gamma_T < \gamma_{q+1}$: (1) monotonically decreasing if $R_q - \mathcal{A}_1 > 0$, which implies $\gamma_T = \gamma_q$ (2) monotonically increasing if $R_q - \mathcal{A}_1 < 0$, which implies $\gamma_T = \gamma_{q+1}$. Hence, the threshold γ_T which maximizes the ASE within bin q is one of the two fading bin endpoints. In Figure 2, $R_q - \mathcal{A}_1$ is depicted as function of $\overline{\gamma}$, $m = 1$, and $q = [1, 2, \ldots, 7]$. It is observed that $R_q - \mathcal{A}_1$

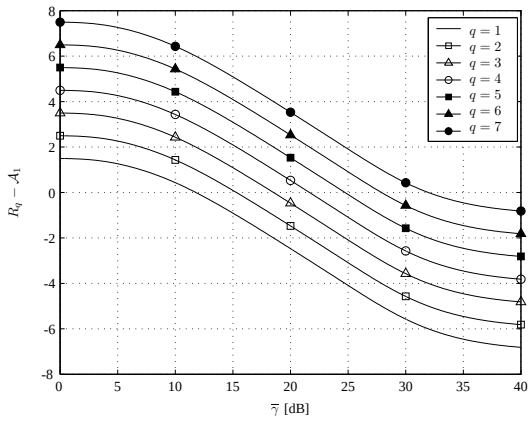


Fig. 2. The size of $R_q - \mathcal{A}_1$ for $m = 1$, governing the sign of the gradient in (7).

is positive at low average SNR and negative at high average SNR. Hence, $\gamma_T = \gamma_q$ for low average SNR, and $\gamma_T = \gamma_{q+1}$ for high average SNR. The switching point between these two solutions, denoted $\overline{\gamma}^*$, can be determined from the equality condition $R_q = \mathcal{A}_1$.[6] Using Newton's method, $\overline{\gamma}^*$ can be determined by means of the recursion in (13) (see next page), where $i = 0, 1, \ldots$ and $\beta_i = \overline{\gamma}^*(i)/m$. The initial value $\overline{\gamma}^*(0)$ can be selected as γ_1. Knowing that the set of thresholds maximizing the ASE within bin q is limited to either γ_q or γ_{q+1}, the optimal threshold γ_T^*, maximizing the ASE among all fading bins, is derived as follows:

$$\gamma_T^* = \gamma_{q^*} \quad \text{where} \quad q^* = \underset{\gamma_T = \{\gamma_q\}_{q=1}^N}{\arg\max} \text{ ASE}. \quad (14)$$

In Figure 4, γ_T^* is depicted as a function of $\overline{\gamma}$ for $m = \{1, 2, 4\}$.

V. Impact of branch correlation

Spatial correlation between the antenna branches may arise e.g. from insufficient antenna spacing in small-size terminals. For identically distributed but spatially correlated Nakagami-m fading channels, the PDF of the output SNR may be written as [7]

$$p_{\gamma_{ssc}}(\gamma) = \begin{cases} \mathcal{G}_\gamma(m, \beta) \cdot (1 - Q_m(\alpha_s \sqrt{\gamma}, \beta_s)) & \gamma \leq \gamma_T \\ \mathcal{G}_\gamma(m, \beta) \cdot (2 - Q_m(\alpha_s \sqrt{\gamma}, \beta_s)) & \gamma > \gamma_T \end{cases}, \quad (15)$$

where $\mathcal{G}_\gamma(m, \beta) = p_\gamma(\gamma)$ in Table I, $Q_m(\cdot, \cdot)$ is the generalized Marcum-Q function, $\alpha_s = \sqrt{\frac{2\rho_s}{(1-\rho_s)\beta}}$, $\beta_s = \sqrt{\frac{2\gamma_T}{(1-\rho_s)\beta}}$, and ρ_s denotes the normalized spatial power correlation coefficient. Using the same type of analysis as presented in Section III,

[5] $\overline{\Gamma}(x, y) = \Gamma(x, y)/\Gamma(x)$ is the normalized complementary incomplete gamma function.

[6] When $\overline{\gamma} = \overline{\gamma}^*$, (7) is equal to zero, and any value for γ_T within the range $\gamma_q \leq \gamma_T < \gamma_{q+1}$ will in fact maximize the ASE.

$$\overline{\gamma}^*(i+1) = \overline{\gamma}^*(i) + \frac{R_q - \mathcal{A}_1}{\sum_{n=1}^{N} R_n \left(\frac{\gamma_n}{\overline{\gamma}^*(i)} \mathcal{G}_{\gamma_n}(m, \beta_i) - \frac{\gamma_{n+1}}{\overline{\gamma}^*(i)} \mathcal{G}_{\gamma_{n+1}}(m, \beta_i) \right)}, \tag{13}$$

closed-form expressions for the ASE the average BER can be derived. However, due to space limitations, the explicit expressions are omitted in this paper.

VI. Numerical results

Numerical results are presented for $\text{BER}_0 = 10^{-4}$, $N = 8$, $\{M_n\}_{n=1}^N = \{4, 8, 16, 32, 64, 128, 256, 512\}$, and $\{R_n\}_{n=1}^N = \{1.5, 2.5, \ldots, 8.5\}$.[7] In Figure 3, the maximum ASE of the SSC combiner is compared to dual-branch MRC and selection combining (SC) when operating on i.i.d. Rayleigh fading channels. For the SSC combiner, the ASE is maximized by

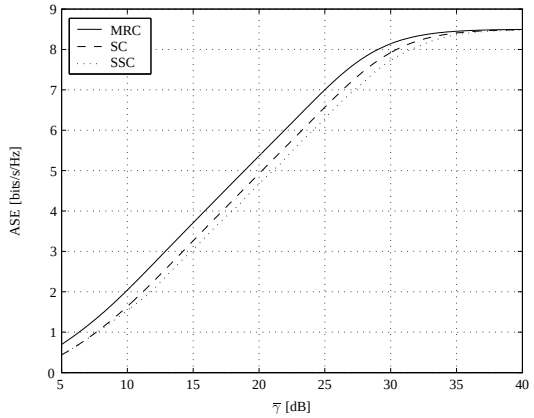


Fig. 3. ASE as a function of $\overline{\gamma}$ when operating on i.i.d. Rayleigh fading channels. For SSC, $\gamma_T = \gamma_T^*$ for each value of $\overline{\gamma}$.

employing the optimal switching threshold γ_T^* for each value of $\overline{\gamma}$. As a result, the performance of SSC is close to the performance of both MRC and SC. In Figure 4, γ_T^* used to generate the SSC curve in Figure 3 is depicted as a function of $\overline{\gamma}$ and the Nakagami-m fading parameter. It is a stepwise function where the discrete values of γ_T^* are identical to the predefined thresholds $\{\gamma_n\}_{n=1}^N$ of the rate-adaptive scheme. As the Nakagami-m parameter is increased, the stepwise function is shifted to the left, reflecting that an increase in γ_T^* occurs at an earlier stage when the channels become more stable.

In Figure 5, the average BER is depicted when operating on i.i.d. Nakagami-m fading channels with $m \in \{1, 2\}$. For SSC, results are depicted when γ_T^* is used as switching threshold. The target $\overline{\text{BER}}_0 = 10^{-4}$ is achieved, and the performance is almost identical to MRC and SC at low and medium $\overline{\gamma}$. Note that the diversity advantage of SSC is lost at high $\overline{\gamma}$. The reason is that γ_T^* is not increased beyond γ_N, the highest threshold of the rate-adaptive scheme. Since the instantaneous SNR easily exceeds γ_N when $\overline{\gamma}$ is large, the switching rate between the

[7]In this paper, the spectral efficiencies $\{R_n\}_{n=1}^N$ are derived from [2, Eq. (2.2)], using a four-dimensional trellis code ($G = 2$).

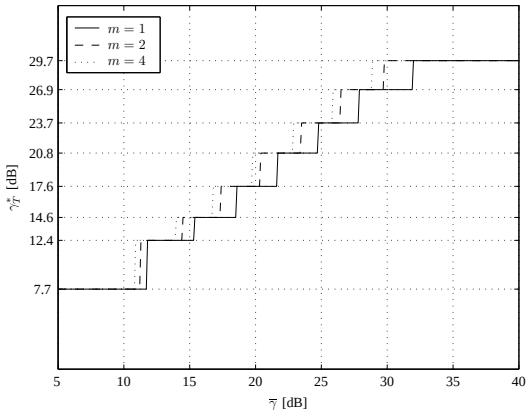


Fig. 4. Switching threshold γ_T^*, maximizing the ASE over all fading bins, as a function $\overline{\gamma}$ and the Nakagami-m fading parameter.

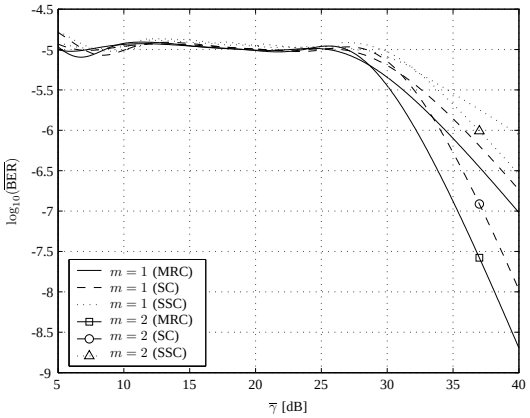


Fig. 5. Average BER as a function of $\overline{\gamma}$ and the Nakagami-m fading parameter. For SSC, $\gamma_T = \gamma_T^*$ for each value of $\overline{\gamma}$.

branches will tend to decrease. When the switching rate is reduced, the SSC receiver approaches a single branch receiver. This effect is reflected in Figure 5 for SSC at high average SNR, since the average BER curves have slopes equal to one and two for $m = 1$ and $m = 2$, respectively. The slopes are then identical to the average BER slopes of a single branch receiver for $m = 1$ and $m = 2$, respectively.

In Figures 6 and 7, the impact of fading correlation is depicted when operating on identically distributed Rayleigh fading channels. The switching threshold γ_T is now chosen to be fixed at $\gamma_T = 17.6$ dB, to illustrate how the performance is affected by not adapting γ_T to $\overline{\gamma}$ on the channels. According to Figure 4, $\gamma_T = 17.6$ dB maximizes the ASE for spatially uncorrelated channels in the vicinity of $\overline{\gamma} = 20$ dB. Indeed, in Figure 6, it is observed that the ASE for spatially uncorrelated channels and $\gamma_T = 17.6$ dB is identical to the maximum ASE

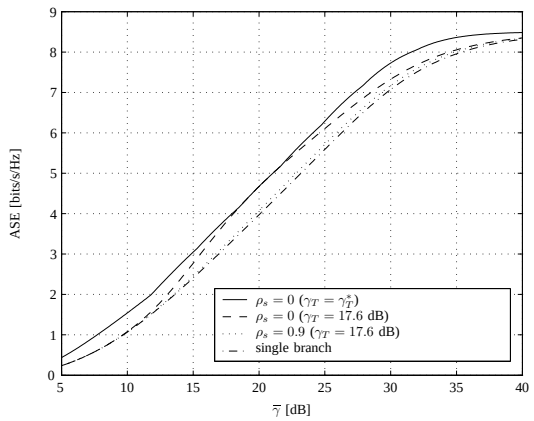


Fig. 6. ASE as a function of $\overline{\gamma}$ and ρ_s when operating on identically distributed Rayleigh fading channels. In the single branch case, ASE $= \mathcal{A}_1$.

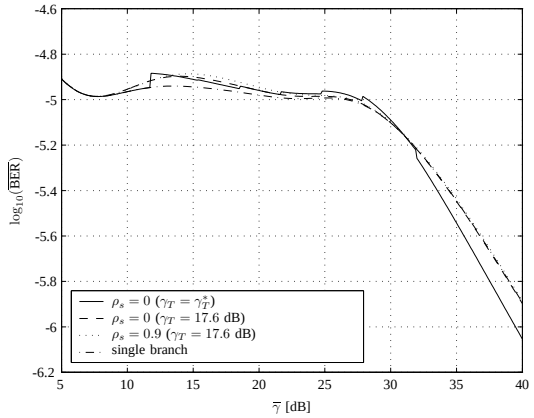


Fig. 7. Average BER as a function of $\overline{\gamma}$ and ρ_s when operating on identically distributed Rayleigh fading channels. In the single branch case, $\overline{\text{BER}} = \mathcal{B}_1/\mathcal{A}_1$.

in this particular SNR region. In addition, it is observed that for $\rho_s = 0.9$, the ASE is reduced, and it approaches the ASE obtained with just a single branch receiver.

From Figure 7, it is concluded that spatial correlation has not a big impact on the average BER performance. When $\gamma_T = 17.6$ dB, the average BER is almost identical to the result obtained by using $\gamma_T = \gamma_T^*$, except at high $\overline{\gamma}$. At high $\overline{\gamma}$, a relatively low and fixed value of γ_T will not be well adapted to the actual channel quality, and the switching process between the branches will then diminish rather then continue. Since $\gamma_T^* > 17.6$ dB at high $\overline{\gamma}$, it contributes to reduce the average BER level compared to the case of $\gamma_T = 17.6$ dB due to a higher switching rate.

VII. Conclusion

A performance analysis of a rate-adaptive dual-branch switched diversity system operating on identically distributed Nakagami-m fading channels has been presented. When using the optimal switching threshold, the performance is close to the performance of both MRC and SC in terms of ASE and average BER, but at a lower complexity. It has also been shown that in order to maximize the ASE for a given average SNR on the channels, the switching threshold γ_T of the switched diversity receiver must be identical to one of the predefined thresholds of the rate-adaptive scheme.

References

[1] K. J. Hole, H. Holm, and G. E. Øien, "Adaptive multidimensional coded modulation on flat fading channels," *IEEE Journal on Selected Areas in Communincations*, vol. 18, no. 7, pp. 1153–1158, July 2000.

[2] H. Holm, "Adaptive coded modulation and channel estimation tools for flat fading channels," Ph.D. dissertation, The Norwegian University of Science and Technology, April 2002 (available at: http://www.iet.ntnu.no/projects/beats/theses.htm).

[3] J. H. Winters, "Optimum combining in digital mobile radio with cochannel interference," *IEEE Transactions on Vehicular Technology*, vol. VT-33, no. 3, pp. 144–155, August 1984.

[4] Y. -C. Ko, M. -S. Alouini, and M. K. Simon, "Analysis and optimization of switched diversity systems," *IEEE Transactions on Vehicular Technology*, vol. 49, no. 5, pp. 1813–1831, September 2000.

[5] M. Blanco and K. Zdunek, "Performance and optimization of switched diversity systems for detection of signals with Rayleigh fading," *IEEE Transactions on Communications*, vol. COM-27, no. 12, pp. 1887–1895, December 1979.

[6] M. Blanco, "Diversity receiver performance in Nakagami fading," *in Proc. IEEE Southeastern Conference*, pp. 529–532, April 1983.

[7] A. A. Abu-Dayya and N. C. Beaulieu, "Analysis of switched diversity systems on generalized-fading channels," *IEEE Transactions on Communications*, vol. 42, no. 11, pp. 2959–2966, November 1994.

[8] ——, "Switched diversity on microcellular Ricean channels," *IEEE Transactions on Vehicular Technology*, vol. 43, no. 4, pp. 970–976, November 1994.

[9] H. -C. Yang and M. -S. Alouini, "Performance analysis of multibranch switched diversity systems," *IEEE Transactions on Communications*, vol. 51, no. 5, pp. 782–794, May 2003.

[10] C. Tellambura, A. Annamalai, and V. K. Bhargava, "Unified analysis of switched diversity systems in independent and correlated fading channels," *IEEE Transactions on Communications*, vol. 49, no. 11, pp. 1955–1965, November 2001.

[11] L. Yang and M. -S. Alouini, "Average level crossing rate and average outage duration of switched diversity systems," *in Proc. IEEE Global Telecommunications Conference*, vol. 2, pp. 1420–1424, November 2002.

[12] G. Femenias, "Reference-based dual switch and stay diversity systems over correlated Nakagami fading channels," *IEEE Transactions on Vehicular Technology*, vol. 52, no. 4, pp. 902–918, July 2003.

[13] N. C. Sagias, D. A. Zogas, G. K. Karagiannidis, and G. S. Tombras, "Performance analysis of switched diversity receivers in Weibull fading," *IEE Electronics Letters*, vol. 39, no. 20, pp. 1472–1473, October 2003.

[14] ——, "Error-rate analysis of switched diversity receivers in Weibull fading," *IEE Electronics Letters*, vol. 40, no. 11, pp. 681–682, May 2004.

[15] H. -C. Yang and M. -S. Alouini, "Markov chains and performance comparison of switched diversity systems," *IEEE Transactions on Communications*, vol. 52, no. 7, pp. 1113–1125, July 2004.

[16] N. Belhaj, N. Hamdi, M. -S. Alouini, and A. Bouallegue, "Low-power minimum estimation and combining with adaptive modulation," *in Proc. IEEE International Symposium on Signal Processing and its Applications*, vol. 2, pp. 687–690, August 2005.

[17] I. S. Gradshteyn and I. M. Ryzhik, *Table of Integrals, Series, and Products*. 5th ed., San Diego, CA: Academic Press, 1994.

[18] M. S. Alouini and A. J. Goldsmith, "Adaptive modulation over Nakagami fading channels," *Wireless Personal Communications*, vol. 13, pp. 119–143, May 2000.